

Article

Potential Loss of Toxic Elements from Slope Arable Soil Erosion into Watershed in Southwest China: Effect of Spatial Distribution and Land-Uses

Ya Gao ¹, Feipeng Li ¹, Lingchen Mao ¹, Bihan Gu ¹, Changkang Peng ¹, Qiuning Yang ², Longchi Lu ², Xilin Chen ², Daofang Zhang ^{1,*} and Hong Tao ^{1,*}

- ¹ School of Environment and Architecture, University of Shanghai for Science and Technology, Shanghai 200093, China; gaoya_sc@163.com (Y.G.); lifeipeng@usst.edu.cn (F.L.); mao.lingchen@usst.edu.cn (L.M.); 15137982132@163.com (B.G.); pck9125@163.com (C.P.)
- ² Water Affairs Bureau of Qiannan, Qiannan 558013, China; yqiuning@126.com (Q.Y.); lulongchi20@163.com (L.L.); cxilin2021@163.com (X.C.)
- * Correspondence: zhangdf-usst@163.com (D.Z.); taohong@usst.edu.cn (H.T.); Tel.: +86-021-55275979 (D.Z.); +86-021-55271991 (H.T.)

Abstract: The watershed-scale distribution and loss of potentially toxic elements (PTEs) through soil erosion from slope lands to a watershed has not yet been systematically studied, especially in small mountain watersheds with high geological background PTEs in Southwest China. In this study, the spatial distribution, loss intensities and ecological risks of 12 PTEs were investigated in 101 soil samples from four types of land use in a typical watershed, Guizhou Province. Moreover, in order to avoid over- or underestimation of the contamination level in such specific geologies with significant variability in natural PTE distribution, the local background values (local BVs) were calculated by statistical methods. The dry arable land had the highest loss intensity of PTEs and was the largest contributor of PTEs (more than 80%) in the watershed, even though it covers a much smaller area compared to the forest land. The loss of Cd, As, Sb, and Hg from slope arable lands into the watershed leads to a relatively high potential ecological risk. The study suggested that both PTEs content with different types of land-uses and intensities of soil loss are of great importance for PTEs' risk assessment in the small watershed within a high geological background region. Furthermore, in order to reduce the loss of PTEs in soil, the management of agricultural activities in arable land, especially the slope arable land, is necessary.

Keywords: slope land; high geological background; potentially toxic elements; loss risk; watershed-scale distribution



Citation: Gao, Y.; Li, F.; Mao, L.; Gu, B.; Peng, C.; Yang, Q.; Lu, L.; Chen, X.; Zhang, D.; Tao, H. Potential Loss of Toxic Elements from Slope Arable Soil Erosion into Watershed in Southwest China: Effect of Spatial Distribution and Land-Uses. *Minerals* **2021**, *11*, 1422. <https://doi.org/10.3390/min11121422>

Academic Editors: Pedro Tume and Maria Economou-Eliopoulos

Received: 4 November 2021

Accepted: 12 December 2021

Published: 15 December 2021

Publisher's Note: MDPI stays neutral with regard to jurisdictional claims in published maps and institutional affiliations.



Copyright: © 2021 by the authors. Licensee MDPI, Basel, Switzerland. This article is an open access article distributed under the terms and conditions of the Creative Commons Attribution (CC BY) license (<https://creativecommons.org/licenses/by/4.0/>).

1. Introduction

Slope arable land is a typical agricultural mode in hilly and mountainous areas in China, which covers about 36.42 million hectares [1]. This type of cultivation suffers from soil erosion and can impact on the water quality of watersheds when contaminated soils are flushed into streams [2]. The slope arable land is famous for its various land uses. Land use changes alter the hydrological process and have significant impacts on the ecological processes by altering the soil erosion patterns and land cover [3]. These ecological processes directly affect the accumulation and migration of the chemical contaminants [4]. One of the most important concerns is potentially toxic elements (PTEs) because of their toxicity, persistence, and non-degradability in nature [5–10]. Zhang et al. [5] found that PTEs are mainly accumulated in the top 0–20 cm of surface soil and easily migrate to human environments. Through the use of chemical fertilizers, compost and manure, and pesticides and herbicides, along with atmospheric deposition and natural contributions, the PTE loads in slope arable soil have been increased substantially, not only affecting the safety

of agricultural products, but also the ecosystem of the whole watershed through soil erosion [6–9].

Southwest China has a humid subtropical monsoon climate, with relatively high annual precipitation (800–1600 mm), which often results in much soil erosion [11]. Besides, strong chemical dissolution from carbonated rocks form karst topography and accelerate the downward leakage of surface water. When scoured by high intensity rainstorms, the surface soil layer with low water content and loose soil is easily to lose. The area also suffers from high PTEs contamination. Current and historical mining has resulted in much PTE (Sb, As, Hg, Cr, Zn, Cd, Pb and Cu) contamination in soils [12,13]. Moreover, it was also found that soils in southwest China often have high geochemical background levels of PTEs, including Cd, As, etc., as a result of higher PTE contents in carbonate bedrock, which easily becomes weathered [14,15]. Generally, it is necessary to use soil background values to judge whether a specific soil is polluted in soil environmental management [16]. The provincial level geochemical background is always preferable for risk assessment rather than using regional/local level geochemical background/standards. However, due to the adverse terrain and geological conditions, the soil in Southwest China is often heterogeneous. Based on regional-scale mapping, Sahoo et al. [17] determined the geochemical background values in soils of the Itacaiúnas River Basin (Brazil), and claimed that site-specific geochemical background must be considered for the accurate evaluation of anthropogenic contamination. A recommended methodology was also issued by the Ministry of Ecology and Environment of China (the statistics of regional environmental background content of soil, HJ 1185—2021) for determining local geochemical background, which was used in this study. Due to limitations imposed by labor costs, most studies have covered large-scale contamination by several PTEs, especially in regions polluted by heavy industry, such as the Yangtze River delta [18] and the Pearl River Delta [19]. Several studies have analyzed the pollution of PTEs in river basins, which are the main agricultural and industrial areas [20]. Current studies about slope arable land mainly focus on soil erosion and loss of nutrients (phosphorus and nitrogen), but the knowledge about PTEs contaminating watersheds via soil loss is limited [21–23]. Very few studies have attempted to study the soil contamination, watershed-scale distribution, and risk of PTEs in a small mountain watershed in Southwest China, although the region is often considered have a high geological background level of PTEs. With the development of agricultural practices in sloping land, the input of PTEs to the soil is increasing. Thus, such ecological environments will be destroyed, and the risk of PTE loss with soil erosion will increase [9]. It is of great significance to study the spatial distribution and loss risks of PTEs in soils to preventing crop pollution and maintaining soil and water quality. However, the watershed-scale distribution and loss risk assessment of PTEs from slope lands to dam fields are ignored so far, and the knowledge about the content, distribution and loss risk of PTEs is deficient in these small mountain watersheds.

In order to develop specific theory and provide data to support for the protection of small watersheds in Southwest China, three issues must be clarified: How the distribution of PTEs in the farmland in a small watershed is closely related to the potential sources of contamination. How do different crops affect the accumulation of PTEs in soil? Will the current status of PTEs, and their loss in relation to soil erosion, affect the regional water environment? We took the Caidi River Watershed, a typical small watershed where a drinking water reservoir is under construction, in Guizhou Province, China, as the study subject. Based on surveys and geographic statistical analysis, the contents, distribution characteristics, and loss risks of 12 PTEs in different land types, especially cultivated land, were studied. This study aims to provide basic data for the treatment of agricultural non-point source pollution in small watersheds and the safety of downstream reservoirs.

2. Materials and Methods

2.1. Study Area and Sampling

The Caidi River Watershed, located in the SW of Duyun City, Guizhou Province in China, belongs to the slope zone from Guizhou Plateau to Guangxi hills. The total area of the Caidi River Watershed is approximately 200 km². The Caidi River has a total length of 45 km with a natural drop of about 700 m and is a rain-source river in mountainous areas. The study area comprises limestone, dolomite, quartz sandstone, shale, marl, clayey siltstone and calcareous shale. There are several soil types within the Caidi River Watershed: zonal yellow soil and non-zonal lime soil, paddy soil and a small amount of fluvo-aquic soil, mountain yellow brown soil, purple soil, red soil, of which yellow soil is the most widely distributed. The main types of landforms are eroded landforms, with local eroded, dissolution landforms, and eroded valley landforms. There are warm conifers and evergreen or deciduous broad-leaved trees, with vegetation coverage of 40%. The main cultivation activities within the watershed are mainly for rice, corn, and tea crops. According to the slope information extracted from the digital elevation data (DEM) provided by the Geospatial Data Cloud (<https://www.gscloud.cn>, accessed on 30 May 2021), more than 90% of the area has slope gradient >5°, with more than 50% greater than 15°. In addition, there is a reservoir under construction in the lower reaches of the Caidi River Watershed (with a storage capacity of about 40 million m³) to supply water to downstream towns and the irrigation of farmland.

Sampling points were randomly arranged according to the regional topography and arable land types, and a total of 101 topsoil samples (0–20 cm) were collected, including 40, 41, 4, 9, and 5 samples from paddy field, corn field, tea plantation, other arable land, and forest land, respectively (Figure 1). When sampling, each sample was a mixture of 5 collections, stored in clean polythene bags and then transported to the laboratory. In the laboratory, soils were air dried, crushed and passed through 10-mesh (2 mm) nylon sieve to remove stones, coarse material, and other debris before analysis.

2.2. Laboratory Analysis

The pH values of soil were measured with a pH meter (FE-20, METTLER TOLEDO, Columbus, OH, USA) according to the potentiometric method with the water-to-soil ratio of 1:2.5. Particle size distribution in soil was determined by laser particle size analyzer (BT-9300Z, Bettersize, Dandong, China). The total organic carbon (TOC) was measured with the method of Soil-Determination of organic carbon—Combustion oxidation nondispersive infrared absorption method (HJ 695–2014). The Hg content was detected by mercury analyzer directly on dry solids (Mile Stone, DMA80, Bergamo, Italy). For other elemental analysis, the samples were ground through 200-mesh (0.075 mm) nylon sieve and then digested (6 mL HNO₃, 3 mL HCl, 2 mL HF) with a microwave digester (Multiwave PRO, Shanghai, China). The content of Cd, Co, Cu, Cr, Ni, Pb, Zn, V, As, Mo and Sb were measured using inductively coupled plasma-mass spectrometry (ICP-MS, PE, NexIon 300X, Irving, TX, USA).

2.3. Establishment of Threshold Background Values and Enrichment Assessment

Considering that Guizhou Province located in a typical high geological background area [5], over/underestimation of level of PTEs contamination is likely using the background values (province-scale BVs) of Guizhou Province [24]. Therefore, background values based on the PTE data from soil surveys in this watershed (local BVs) were also calculated by the statistical calculation of local background values (HJ 1185–2021), which includes the acquisition of the environmental background data of the sampled local soils, data processing (test of distribution types, identification, and processing of outliers), and then data statistics and characterization.

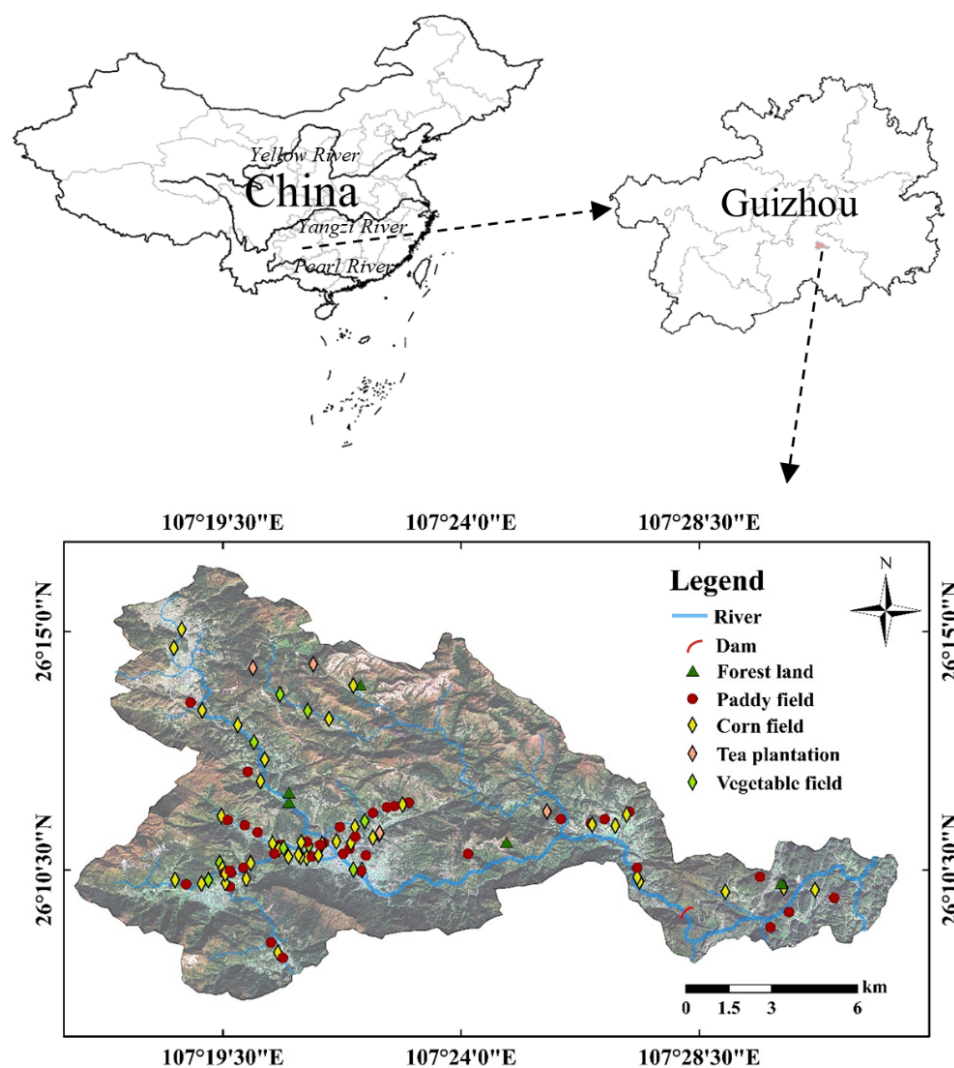


Figure 1. Sampling locations in the Caidi River Watershed, Guizhou Province.

The calculation results and characteristics of the calculated background values are shown in Table S1. Both province-scale BVs and local BVs were used as background values to participate in the following evaluation of the PTEs enrichment and ecological risks in the soil, and comparisons were also made.

Introduced by Müller [25], geo-accumulation index (I_{geo}) is a commonly used assessment model for assessing PTEs pollution in soils using Equation (1):

$$I_{geo} = \log_2[C_i / (k \times B_i)], \tag{1}$$

where C_i is the content of measured metal “ i ” in the samples, B_i is the background content of the metal “ i ” employing the background content in soils. The k is a constant valued 1.5 acting as the background matrix correction due to lithospheric effects to minimize the variation of background values. The index of geo-accumulation consists of seven classifications: unpolluted (<0), unpolluted to moderately polluted (0–1), moderately polluted (1–2), moderately to severely polluted (2–3), severely polluted (3–4), extremely severely polluted (4–5), and extremely polluted (>5) [26].

The potential ecological risk index (RI) was developed to assess ecological risks from the elements in sediments [27]. In this study, it was used to estimate the ecological risk of PTEs flushed from soil to the watershed. The methodology is based on the assumption

that the sensitivity of an aquatic system depends on its productivity and can be calculated by Equations (2)–(4):

$$C_f^i = C_D^i / B_i, \quad (2)$$

$$E_r^i = T_r^i \times C_f^i, \quad (3)$$

$$RI = \sum_{i=1}^m E_r^i, \quad (4)$$

where C_f^i is the contamination factor; C_D^i is the metal content in soil; B_i is the background value which is also used in the I_{geo} calculation aforementioned. T_r^i is the toxic response factor for a given metal: for Cd, Cu, Cr, Pb, Zn, As, Hg and Sb, the factors are 30, 5, 2, 5, 1, 10, 40 [28], and 7 [29]. E_r^i is the potential ecological risk of single PTE, which is graded as: low ($E_r^i < 40$), moderate ($40 \leq E_r^i < 80$), considerable ($80 \leq E_r^i < 160$), high ($160 \leq E_r^i < 320$), or very high ($E_r^i \geq 320$); RI is calculated as the sum of potential risk of single PTE, and classified as low risk ($RI < 150$), moderate risk ($150 \leq RI < 300$), considerable risk ($300 \leq RI < 600$), or very high risk (≥ 600).

2.4. Calculation of Soil Erosion and PTE Loss

The amount of soil erosion within the Caidi River Watershed was evaluated on the GIS platform based on the Revised Universal Soil Loss Equation (RUSLE) [30]. The RUSLE was developed from the Universal Soil Loss Equation (USLE) [31], which considered rainfall, soil erodibility, topography, cover management, and support practice as important factors affecting soil erosion (Equation (5)). In this study, Arc GIS was used to establish a basic database, and the Raster Calculator module was used to perform graphical operations to realize water erosion prediction and erosion intensity evaluation. The potential amount of soil erosion (AP) was also calculated, which refers to the average annual soil loss when there is no vegetation cover and soil erosion control measures (Equation (6)) [32]. The amount difference between potential soil erosion and soil erosion under current land use or cover condition is the amount of soil retained by the control measures (soil retention). In addition, we used the empirical model of spatial distribution, ratio of sediment delivered (SDR), and measured contents of PTEs to calculate the sediment yields (Equation (7)) [33] and the amounts of PTEs exported to the river along with soil erosion (Equation (8)) [34]. The method based on RUSLE and SDR can calculate the lost soil flux, the regional source of the sediment yield, and evaluate the impacts of land use types, water, and soil conservation measures on the erosion modulus and sediment yield [35,36].

$$A = R \times K \times LS \times C \times P, \quad (5)$$

$$AP = R \times K \times LS, \quad (6)$$

$$S = A \times SDR, \quad (7)$$

$$Q_i = A \times SDR \times C_i \times 10^{-6}, \quad (8)$$

where A refers to annual soil loss ($t/(hm^2 \cdot a)$); AP refers to potential amount of soil erosion ($t/(hm^2 \cdot a)$); S refers to sediment yield ($t/(hm^2 \cdot a)$); Q_i refers to annual soil loss of PTEs ($kg/(hm^2 \cdot a)$); R refers to rainfall erosivity factor ($MJ \cdot mm/(hm^2 \cdot h \cdot a)$) [37] and the rainfall data was obtained from <http://data.cma.cn> (assessed on 30 May 2021); K refers to soil erodability factor ($t \cdot h/(MJ \cdot mm)$) [38]; LS refers to slope length factor \times slope steepness factor [39,40]; $C \times P$ refers to cover-management factor (C) \times supporting practices (P) [41], the land use data were acquired from National Geomatics Center of China (<http://www.globallandcover.com>, accessed on 1 June 2021) and field survey; C_i refers to content of PTEs (mg/kg) in soil; SDR refers to sediment delivery ratio [42].

2.5. QA/QC

The quality assurance and quality control (QA/QC) procedures were performed by setting blank and quality control samples for each batch of soil sample. Laboratory

contamination was not detected during analysis according to the low content (less than detection limit) in reagent blanks. The standard materials of GBW07455 (GSS-26) and GBW07453 (GSS-24) were set as references for quality control in the digestion process and the recovery rates were 80.6%–89.1% and 81.0%–89.4%, respectively. The standard reference material of Hg (ESS-3, GSBZ50013-88), from the China National Environmental Monitoring Centre, was analyzed, and the recovery was in the range of 93.4%–112%. In the process of PTEs content analysis, replicates were measured every 5 samples, and the relative error was $\leq 10.7\%$. Duplicates were made for all Hg analysis with $RSD \leq 12.6\%$. When determining by ICP-MS, each sample was analyzed 3 times, and the relative standard deviation was $\leq 11.8\%$. For trace elements analysis, internal standards, including Ge (10 $\mu\text{g/L}$), In (5 $\mu\text{g/L}$) and Bi (5 $\mu\text{g/L}$), were particularly introduced to the sample stream via a T-piece to correct the matrix differences between the calibration standards and samples, so that the accuracy of the results can be largely improved.

2.6. Statistical Analysis

Statistics analysis and mapping of data were carried out by using Excel 2019 (Microsoft, Redmond, WA, USA) and SPSS 26.0 (IBM, Chicago, IL, USA) and Origin 2018 (Origin Lab, Northampton, MA, USA). ArcGIS 10.6 (ESRI, Redlands, CA, USA) was utilized to describe the spatial distribution and the calculation of soil erosion and loss of PTEs.

3. Results

3.1. Physicochemical Properties and Content of PTEs in Soil

Table S2 shows the pH values, particle sizes, and total organic carbon (TOC) content of the soil samples collected in the Caidi River Watershed. The sampled soils were generally weakly acidic, with pHs from 4.56 to 8.04 and an average value of 6.37. The soil textures were mainly silty loam and sandy loam. The TOC content of soil samples were between 9.79–82.83 g/kg, with an average of 36.24 g/kg.

Table 1 shows the contents, background values (both province-scale BVs and local BVs), and comparisons of the 12 PTEs in the soil samples: the average contents of Cd, Co, Cu, Cr, Ni, Pb, Zn, V, As, Mo, Sb, and Hg were 0.4, 5, 14, 33, 13, 20, 67, 51, 11, 1, 4.3, and 0.34 mg/kg, respectively. The coefficient of variation (CV) order of PTEs is: Sb > Hg > As > Zn > Mo > Cd > Co > Ni > Cu > V > Cr > Pb. Particularly, Sb and Hg have larger coefficients of variation (2.58 and 1.73), whose content ranges are 0.6–92 and 0.01–3.62 mg/kg, respectively, indicating that the two metals may have local pollution.

Relatively high Sb, Hg, Cd, As, Zn were generally found in Caidi River Watershed. The average contents of Sb and Hg exceed the corresponding province-scale BVs, which were 1.9 and 3.1 times of the corresponding province-scale BVs, while the other metals are below province-scale BVs. The maximum contents of the tested metals (except Co) exceed the corresponding province-scale BVs. The maximum values of Sb and Hg are significantly 41 and 33 times that of province-scale BVs, and Zn, As and Cd are 4.2, 3.2 and 2.3 times that of province-scale BVs, respectively. As to local BVs, the average contents of Sb and Hg are 2.7 and 1.8 times that of local BVs, and the average contents of other metals are slightly higher. The maximum values of Sb and Hg are 58 and 21 times that of local BVs, and Zn, As, Mo, Cd, Ni and Cu are 6.3, 7.9, 5.5, 4.7, 4.7 and 4.3 times that of local BVs, respectively. There are 44% of sites where Cd exceeds risk screening value (RSV) (GB 15618-2018), and the average Cd content also exceed the risk screening value of Cd. There are 2, 4 and 6 sites where Zn, As and Hg exceed the corresponding risk screening values. The contents of Cr, Ni, Cu and Pb do not exceed the risk screening values in all the sites. Cd content in soil of this study is higher than the average values of the two provinces (Jiangsu and Zhejiang) in the Yangtze River Basin of China [43], which have generally considered as heavily contaminated by PTEs from industries, but lower than the province-scale BV and other areas in Guizhou provinces, such as the Caohai Wetland area [44] and soil samples from other mining areas [45]. The average contents of Cd, Hg and As in this study (0.4 mg/kg, 0.34 mg/kg and 11 mg/kg) are higher than the average

values of Chinese soils measured in the past 20 years, while the average values of Cu, Cr, Ni, Pb and Zn are lower [46].

Table 1. Total contents of potentially toxic elements in soils from Caidi River Watershed and values from other studies (mg/kg).

	Cd	Co	Cu	Cr	Ni	Pb	Zn	V	As	Mo	Sb	Hg
Max	1.5	15	53	102	55	56	419	169	65	3.1	92	3.6
Min	0.1	1	2	14	2	10	8	25	0.2	0.2	0.6	0.01
Mean	0.4	5	14	33	13	20	67	51	11	1.0	4.3	0.3
SD	0.22	2.82	6.87	11.65	6.86	6.17	50.14	18.81	9.79	0.42	11.03	0.59
CV	0.59	0.58	0.50	0.35	0.53	0.31	0.75	0.37	0.89	0.64	2.58	1.73
Province-scale BVs [28]	0.66	19.2	32	95.9	39.1	35.2	99.5	138.8	20	2.4	2.24	0.11
Local BVs	0.32	4.07	12.36	31.88	11.6	19.25	66.53	47.91	8.2	0.56	1.60	0.17
RSVs (paddy field) *	0.4	-	150	250	70	100	200	-	30	-	-	0.5
RSVs (other land types) *	0.3	-	50	150	-	90	-	-	40	-	-	1.8
China [46]	0.19	-	25.81	67.37	27.77	30.74	85.86	-	8.89	-	-	0.07
Farmland soil in China [46]	0.18	-	25.73	66.81	27.67	30.24	83.87	-	8.45	-	-	0.07
Zhejiang Province [43]	0.23	-	23.96	47.84	21.31	36.79	91.39	-	-	-	-	0.12
Jiangsu Province [43]	0.18	-	29.68	71.49	29.68	28.8	75.87	-	-	-	-	0.07
Caohai Wetland [44]	2.68	-	24.9	89.7	-	22.4	163	-	-	-	-	0.2
Soil in a coal mine zone [45]	1.09	-	134.09	173.63	64.89	240.61	-	-	477.58	-	-	0.71

* Risk screening values (RSVs) refer to the limit values when the pH is 5.5–6.5 regulated in Soil Environmental Quality—Risk Control Standard for Soil Contamination of Agricultural Land (GB 15618–2018). “-” means no data.

The geo-accumulation index (I_{geo}) was calculated and classified based on both province-scale BVs (open circle) and local BVs (closed circle), separately, as shown in Figure 2. The pollution status is: Hg > Sb > Zn > Pb > Cd > As > Cu > V > Cr > Ni > Mo > Co. More than 60% of sites were contaminated by PTEs to different extents ($I_{geo} > 0$), among which about 22% and 10% of sites were moderately to strongly contaminated ($I_{geo} > 1$) by Hg and Sb, respectively. According to the calculated local background values of I_{geo} , the level of contamination is generally higher than what was found in Guizhou province-scale BVs, except for Hg. Taking Cd as an example, when calculating the background value based on the local samples, the numbers of slightly polluted and moderately polluted sites increase by 15 and 2, respectively. Similarly, the evaluation of Sb has also changed greatly: the numbers of sites showing serious pollution, moderate pollution, and light pollution increase by 1, 2, and 6, respectively. This result implies that variability in background values of PTEs in southwest China is significant, which may lead to biases in assessment result.

3.2. Spatial Distribution of PTEs and Effect of Land Use

Figure 3 shows the spatial distributions of PTEs in the Caidi River arable soils. The variations in distribution among different PTEs indicate the impacts of sources on the spatial distributions of PTEs. Hg and Sb show obvious partial enrichment trends concentrated in the SW area near Jiangzhou Town. The sites with high contents of Zn, Pb, and Cd are generally located in the east of the watershed and the upper reaches of the reservoir. Cd and Pb also have higher contents in the downstream and western area, presenting a characteristic of widespread pollution. The highest content of As is in the SW of the watershed, and there are also high contents in the northern area and the upper reaches of the reservoir.

It is worth mentioning that there are obvious enrichment areas for Sb, whose content is much higher than that of local BVs. At present, there are few studies on antimony in the soil in southwestern China, and most of them are associated with mining activities [45,47]. Although the Sb concentrations we found were less than those found the soil near mining areas in previous studies [48,49], the still high Sb concentrations may be attributed to a mercury and antimony ore field to the south of Jiangzhou Town.

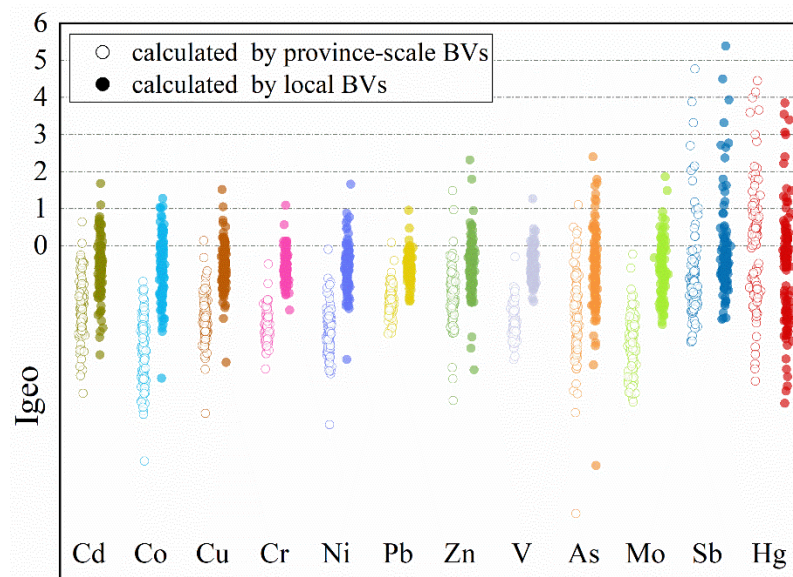


Figure 2. Levels of PTE contamination classified by I_{geo} in the Caidi River Watershed. Each group of open circles or closed circles represents the geo-accumulation index (I_{geo}) of one PTE: Cd (bronze green), Co (baby blue), Cu (brown), Cr (pink), Ni (pale blue), Pb (yellow), Zn (vivid green), V (mauve), As (orange), Mo (grass green), Sb (royal blue) and Hg (red). The open circles and closed circles represent the geo-accumulation indexes calculated based on province-scale BVs and local BVs, respectively.

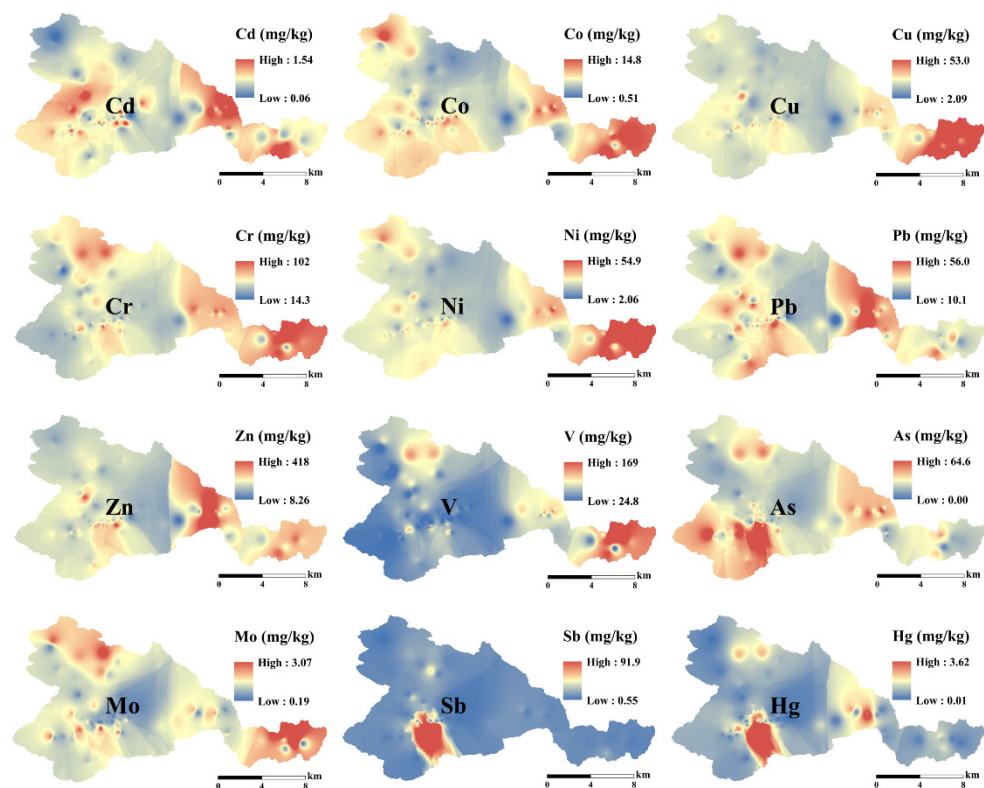


Figure 3. Spatial distributions of PTEs in the soil of the Caidi River Watershed.

The contents of PTEs in soils with different land uses are presented in Table 2. The contents of PTEs in both corn and paddy fields are generally higher than in the other types of land use, and the average contents of Cd, Co, Cu, Cr, Ni, Pb, Zn, and V in these two

land types are relatively close. The average contents of metals that pose high potential ecological risks, such as As, Sb, and Hg, in dry land are significantly higher than those in paddy fields. The order of Sb content by land type is: corn field > paddy field > vegetable field > tea plantation > forest land. The average Sb content in corn fields was 6.4 mg/kg, and the contents in soils from other land types did not exceed 3 mg/kg. The Hg contents in the corn fields and tea plantations were higher than those in the paddy fields, vegetable fields, and forest land. Meanwhile, the average content of Cd in the paddy fields was slightly higher than in the other types of land. The average As content in the paddy fields was 8.19 mg/kg, which was much lower than that in the corn fields (14 mg/kg); there was a significant difference in the As content between the soils of the two crops ($p < 0.01$).

Table 2. The PTE contents in soils from different types of land in the Caidi Watershed (mg/kg).

Metals	Dry Arable Land			Paddy Field	Forest Land
	Corn Field ($n = 41$)	Vegetable Field ($n = 9$)	Tea Plantation ($n = 4$)	Paddy Field ($n = 40$)	Forest Land ($n = 5$)
Cd	0.4 (0.1–1.5)	0.3 (0.2–0.4)	0.2 (0.1–0.4)	0.4 (0.1–0.8)	0.3 (0.1–0.4)
Co	6 (2–15)	3 (1–6)	4 (2–6)	5 (2–13)	2 (1–3)
Cu	14 (6–53)	12 (8–17)	9 (5–13)	14 (7–38)	11 (2–30)
Cr	32 (14–71)	33 (22–51)	44 (26–51)	32 (19–52)	46 (20–102)
Ni	13 (6–32)	9 (6–17)	12 (7–17)	13 (6–28)	15 (2–55)
Pb	20 (11–40)	19 (17–28)	21 (10–28)	20 (11–56)	17 (10–28)
Zn	68 (15–292)	52 (29–74)	42 (12–63)	73 (31–419)	49 (8–92)
V	50 (25–97)	51 (312–77)	63 (33–77)	48 (26–88)	75 (38–169)
As	14 (3–65)	8 (0.2–18)	14 (5–18)	8 (1–22)	10 (6–17)
Mo	0.7 (0.2–3.2)	0.6 (0.3–1.4)	0.9 (0.3–1.4)	0.5 (0.2–1.4)	1 (0.8–1.6)
Sb	6.4 (0.6–92)	2.7 (1.1–6.8)	2.4 (0.8–3.2)	2.9 (0.6–33.6)	2.1 (1.4–4.0)
Hg	0.44 (0.02–3.62)	0.26 (0.07–0.62)	0.45 (0.03–0.62)	0.26 (0.01–2.09)	0.24 (0.05–0.42)

“ n ” means number of soil samples of each land type.

In this study, there was significant difference in soil particle size between the paddy fields and corn fields. The soil from dry land had a higher clay percentage ($p < 0.05$), indicating more adsorption of PTE cations. Different cultivation practices may also affect PTEs' enrichment. The study by Tu et al. [50] reported that most of the PTE content in paddy field soil was higher than that in dry land soil, and the reason may be that paddy fields receive much more organic fertilizer and less soil erosion, and thus more accumulation. However, a longer farming history and more phosphate fertilizer in dry arable land could also result in a higher accumulation of PTEs in dry land than paddy fields [51]. In this study, it was found that the amount of fertilizer applied to the paddy fields in the study area was less than that to the dry land, which also explains the slightly lower PTE content in paddy soils.

3.3. The Soil Erosion and the Risk of PTE Loss

An analysis of soil erosion and the risk of PTEs carried by soil flow into the watershed was conducted in order to explore the impact of the PTE loss on the regional aquatic environment. The average soil erosion risk of the Caidi River Watershed is 0.28 t/(ha.a), implying slightly erosion in this area with reference to the Chinese standard for classification and grade of soil erosion (SL 190–1996) [52]. For further exploration the impact of human activities and crop types on soil erosion—that is, the soil loss under current land use/cover conditions—we unified the corn, tea, and vegetable fields as dry arable land, and divided it into sloped dry land (slope > 6°) and flat dry land (slope < 6°), and then calculated the soil loss, potential soil loss, and soil retention of each land type (Table 3).

Table 3. The soil erosion of different land types in the Caidi River Watershed.

Land Use Type	Area Proportion	Soil Erosion Risk	Annual Soil Loss	Potential Soil Loss	Soil Retention
	%	t/(ha.a)	t/a	t/a	t/a
Paddy field	14.2%	0.02	36	14,173	14,138
Dry arable land (slope $\leq 6^\circ$)	3.8%	0.69	410	2464	2054
Dry arable land (slope $> 6^\circ$)	10.2%	2.03	3235	11,331	8096
Forest land	67.2%	0.05	535	89,095	88,561
Grassland	4.6%	0.27	194	3241	3046
Total			4410	120,305	115,896

Among the different types of land in the watershed, forest land accounts for the largest proportion (67.2% of the area), followed by paddy fields, dry arable land (slope $> 6^\circ$), grassland, and flat dry arable land (slope $< 6^\circ$). Dry arable land (slope $> 6^\circ$) has the largest erosion intensity and erosion flux of 3.235 t/a apparently, despite its relatively small proportion in the area. The forest land has an erosion flux of only 535 t/a, resulting from the low erosion intensity, despite accounting for the most potential erosion. The paddy field has the smallest erosion rate (36 t/a). The amount of soil conservation is the difference between the potential and current soil erosion, i.e., the amount of soil erosion reduced due to vegetation coverage and the implementation of land management measures [35]. The calculated soil conservation of the Caidi River Watershed accounts for 96.3% of the total potential erosion, which is significantly higher than 63.6% in the Loess Plateau [31]. This may result from the large percentages of forest land and paddy fields. From the perspective of soil conservation, paddy fields have the best soil conservation effects compared with other types of land use. Table S3 lists the PTE loss intensities of different types of land. The intensity of PTE loss in dry arable land (slope $> 6^\circ$) is the highest, followed by dry arable land (slope $\leq 6^\circ$). Grassland has a higher PTE loss intensity than forest land. Paddy field has the lowest PTE loss intensity.

A comparison of the annual losses of PTEs in different types of land is shown Figure 4. The annual loss in dry arable land (slope $> 6^\circ$) accounted for 61.5%–70.3%, while the annual loss in dry arable land (slope $\leq 6^\circ$) and forest land accounted for approximately 12.5%–17.3% and 12.8%–18.0%, separately. The annual loss of metals in paddy fields was the least, only 1.0%–1.5%. It can be concluded that from the loss view, paddy fields with the lowest loss intensity and annual contributions of PTEs may delay the risk of PTE loss from soil erosion to the downstream. Nonetheless, PTEs could accumulate in a paddy field during agricultural activities and then enhance the ecological risk and the health risk from another pathway.

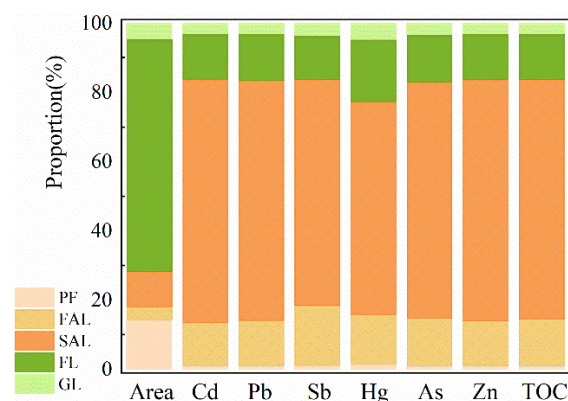
**Figure 4.** The proportions of annual PTE loss in different land types (PF: paddy field, FAL: dry arable land (slope $\leq 6^\circ$), SAL: dry arable land (slope $> 6^\circ$), FL: forest land, GL: grassland).

Figure 5 shows potential ecological risk of PTEs in Caidi River Watershed. RI in all sites range from 18 to 1455, with an average value of 167. 16 sites have moderate potential ecological risk ($RI > 150$), and 9 sites show high or very high potential ecological risk ($RI > 300$). The order of potential ecological risk of single PTEs is: $Hg > Sb > Cd > As > Pb > Cu > Cr > Zn$. The potential ecological risk of Hg, in particular, exceeds 40 in more than half of the sites, and 7% of the sites present very high risks. In general, Cu, Cr, Pb and Zn have lower potential ecological risks. The metals that contribute the most to RI are Hg (in 94 samples), Cd (in 4 samples) and Sb (in 1 sample). The potential ecological risk of Hg in each site has good consistency with the corresponding RI ($R^2 > 0.98$). Similarly, increases have seen in the ecological risks of most PTEs when calculating with local BVs.

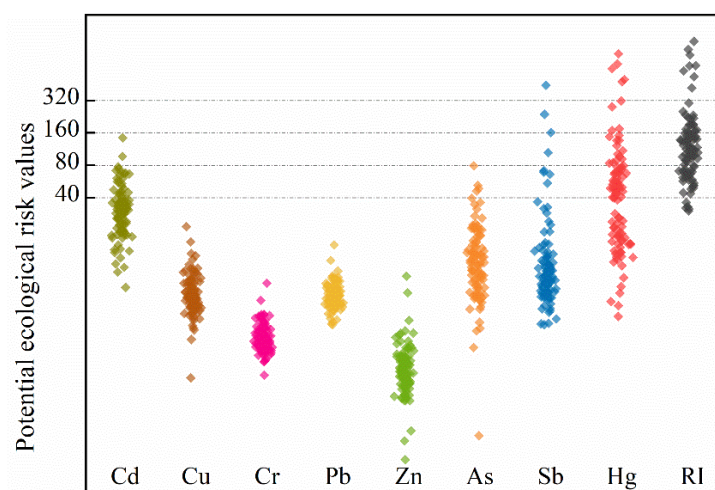


Figure 5. Pollution levels of PTEs classified by E_i^p and RI in the Caidi River Watershed. Each column of little squares represents the potential ecological risk value of one PTE: Cd (bronze green), Cu (brown), Cr (pink), Pb (yellow), Zn (vivid green), As (orange), Sb (royal blue), Hg (red), and RI (black).

4. Discussion

4.1. Importance of Using Local Background Value for PTE Risk Assessments

The PTE background content in soil is confined relative to time and space, and reflects the underlying geology and soil formation processes [53,54]. There is an important metallogenic zone (Sandu-Danzhai) southeast of the study area, which leads to high PTEs contents in both bedrock and soils generated from it [55]. Previous study has found that Cd exhibits the largest ecological risk in the Yungui region, which can be mainly attributed to the high geological background values in this area [56]. Study has also shown that the average contents of Cd, Pb, and As in soils were recently 0.577 ± 0.690 mg/kg, 35.5 ± 36.0 mg/kg, and 19.7 ± 17.1 mg/kg, without obvious anthropogenic input, in the paddy soils of Guizhou Province [14]. Due to the significant variability in natural PTEs distribution, a single threshold value of background content calculated on the provincial scale can potentially over/underestimate PTE enrichment in soils. According to statistics from 1990, the mean cadmium content in soil in Guizhou was 0.66 mg/kg, which is far higher than the national mean content of 0.097 mg/kg [24], and is also significantly higher than the limit of the risk screening value for soil contamination of agricultural land (0.4 mg/kg, when $5.5 < pH \leq 6.5$) stipulated in the Soil Environmental Quality Risk Control Standard for Soil Contamination of Agricultural Land (GB15618–2018). In this study, the local background value of Cd was 52% less than the province-scale BV which was calculated on a $595 \text{ km} \times 509 \text{ km}$ grid covering more than 17 million hectares. It is obvious that if the widely accepted and province-based BV serves as the background value of Cd (0.66 mg/kg) in this area, it will bring about relatively small and conservative conclusions to the assessments of metal accumulation and risk evaluation. This can also happen with the other 10 PTEs, except for Hg, as the local BVs are 28% to 79% less than the regional background values (province-scale BVs). Hence, when conducting soil PTE risk

assessments in relatively clean and small watersheds within areas with high background values, if province-scale BVs (mostly higher regional background values) are used as background values in the calculations, the evaluation results for agricultural health risk analysis and water quality safety assurance could be unscientific and worthy of revision.

This study used local BVs to eliminate the aforementioned bias. Similarly, for the drinking water source protection zone whose risk assessment is extremely strict, the setting of background values, as a key component of assessments of local PTE ecological risks, has a significant impact on the potential risk assessment results. For a PTE presenting a potential risk in analogous area, if a higher background based on a provincial value is adopted, the risks of these elements may be underestimated unintentionally.

Comparing the results calculated based upon the two background values, the potential ecological risks of single metals (except for Hg) obtained by local BVs were elevated, as were the corresponding ecological hazards. In this study, the number of sites with moderate ecological risks of As in the sites rose by four; meanwhile, the increments in sites with strong and moderate Cd ecological risks were 2 and 20 separately, indicating that using local BVs are more likely to find out the potential risk source. In summary, local/regional background values established on a more detailed/small scale should be used in study areas with peculiar geology, e.g., karst tomography in Southwest China, because of their high variability of natural/geogenic PTE distribution, when conducting pollution analyses and ecological risk assessments.

4.2. Risk of PTE Loss from Soil within a Watershed

In the research on slope arable land in mountain watershed, one of the hotspots is soil loss and its impact downstream. In previous studies, the main concerns was the soil erosion rate of slope arable land and the corresponding losses of nutrients and organic matter in the soil [21,54]. However, little attention has been paid to PTEs that migrate with soil erosion. In the process of soil erosion by water in slope arable land, PTEs are strongly adsorbed to soil particles and colloids, for instance, organic matter, and clay, and thus often move with fine particles and carbon in the soil, which in turn causes PTEs to accumulate in the downstream sediments. Quinton et.al. found that the content of PTEs in sediments can be up to 13.5 times those in the parent soils due to erosion events, through field observations over a period of six years, and pointed out that erosion could enrich the detached materials in silt, clay, and organic carbon, especially in smaller erosion events [57]. Accordingly, it is necessary to study the erosion and loss of PTEs in the soil of slope arable land.

Due to disparities in the vegetation, tillage, irrigation, and other practices, the level of soil erosion varies among areas with different land uses. Compared with forest land and grassland, the soil erosion of arable land is often much more serious [58–60]. The calculation of soil loss in the Caidi River Watershed found that the soil loss of dry slope farmland is much higher than in the other types of land. Growing rice on sloped farmland is a common practice in southwest China. In this study, although dry slope farmland had the strongest soil erosion and largest metal loss, the amounts of soil loss and PTE loss in paddy fields were relatively low. It can be deduced that growing rice on sloped farmland has decelerated the loss of PTEs into the watershed to a certain extent. However, considering the rotation of rice and corn in regional planting, the content, distribution, and loss of PTEs in the two types of land are also worthy of attention.

The analysis of PTEs in different land types showed that PTEs with higher risks, such as Cd, As, Pb, and Hg, present higher contents in dry arable land and paddy fields than in forest land, indicating that agricultural activities have possibly resulted in the accumulation of PTEs in arable land. Furthermore, it was found that this accumulation is continuous [61]. Obviously, the accumulation of PTEs caused by agricultural activities on slope arable land, under the influence of rotations in land use and crop types, would accompany the soil loss and then pose risks to the in river-reservoir system downstream. Shown in the spatial distribution of PTEs in the Caidi River Watershed, although mainly distributed in the upper reaches of the reservoir, higher contents of As and Cd may have an impact on

the accumulation of PTEs in the reservoir downstream under the effects of agricultural activities and erosion. Consequently, the control of agricultural activities in the area should be strengthened.

In addition, more than half of the Caidi River Watershed is forest land, which is inaccessible and less managed. The organic carbon input with plant litter and root exudates will significantly increase the soil organic carbon of forest land [62], and the increase in soil organic matter has a direct impact on the adsorption and enrichment of PTEs [63,64]. In view of the high geological background of the watershed, PTEs may also accumulate in the forest soil, and then migrate with water and soil erosion. Therefore, the accumulation of PTEs in the forest land should not be ignored either.

5. Conclusions

This study investigated the spatial distribution, level of contamination, and loss risks of 12 PTEs in different types of land in the Caidi River Watershed in southwest China. The results found that there is significant enrichment of Sb, Hg, Cd, Zn, and As in the soils; Hg and Sb were at high levels in farmland soils. In particular, attention should be paid to the relatively high accumulation of elements such as Sb, Hg, Cd, and As. The high level of Cd in the soils, which is above the risk screening level, were widely distributed. High contents of As and Cd were found in the upstream area, which may have an impact on the water quality of the reservoir downstream. The potential ecological risk analysis showed that Sb, Cd, and As present moderate or even strong ecological risks in some areas. The arable land in the watershed, especially the dry slope land, showed the most loss of PTEs, much more than the forest land (the largest proportion of land). The dry arable land is the main source of PTE loss in the watershed. Although the loss of PTEs in paddy soil was the smallest, the continuous accumulation of PTEs caused by agricultural activities should attract more attention. In addition, this study showed that when investigating the pollution and ecological risks of an area with high geological background levels, it is necessary to reexamine and analyze the regional background values and evaluate the erosion risk in relation to PTEs in the soil. Furthermore, strengthening the management of agricultural activities in arable land, especially the dry slope land, is necessary to reduce the loss of PTEs in farmland soil.

Supplementary Materials: The following are available online at <https://www.mdpi.com/article/10.3390/min11121422/s1>. Table S1: The calculation results of the calculated background values of PTEs. Table S2: The pH values, particle size compositions, total organic carbon (TOC) in soils in the Caidi River Watershed. Table S3: The intensities of metal loss of different types of land in the Caidi River Watershed.

Author Contributions: Conceptualization, Y.G., H.T., F.L. and D.Z.; methodology, Y.G. and C.P.; formal analysis, Y.G.; investigation, B.G., C.P., Q.Y., L.L. and X.C.; writing—original draft preparation, Y.G.; writing—review and editing, F.L. and L.M.; visualization, Y.G. and B.G. All authors have read and agreed to the published version of the manuscript.

Funding: This work was funded by Water Affairs Bureau of Qiannan, Guizhou Province, China (NO. JCZB2019042FW).

Acknowledgments: We thank the Water Affairs Bureau of Qiannan and Guizhou Survey and the Design Research Institute for Water Resources and Hydropower for the help with soil sampling and data collection.

Conflicts of Interest: The authors declare no conflict of interest. The authors declare that they have no known competing financial interests or personal relationships that could appear to have influenced the work reported in this paper.

References

1. Ministry of Land and Resources, National Bureau of Statistics of China, Leading Group Office for Second National Land Survey of the State Council. Bulletin on the main data results of the second National Land Survey. *Resour. Habitat Environ.* **2014**, *1*, 16–17.
2. Sharma, A.; Tiwari, K.N.; Bhadoria, P.B.S. Effect of land use land cover change on soil erosion potential in an agricultural watershed. *Environ. Monit. Assess.* **2011**, *173*, 789–801. [[CrossRef](#)]
3. Shi, P.; Zhang, Y.; Li, P.; Li, Z.; Yu, K.; Ren, Z.; Xu, G.; Cheng, S.; Wang, F.; Ma, Y. Distribution of soil organic carbon impacted by land-use changes in a hilly watershed of the Loess Plateau. *China. Sci. Total Environ.* **2019**, *652*, 505–512. [[CrossRef](#)] [[PubMed](#)]
4. Jarsjö, J.; Chalov, S.R.; Pietroń, J.; Alekseenko, A.V.; Thorslund, J. Patterns of soil contamination, erosion and river loading of metals in a gold mining region of northern Mongolia. *Reg. Environ. Chang.* **2017**, *17*, 1991–2005. [[CrossRef](#)]
5. Zhang, H.; Liu, G.; Shi, W.; Li, J. Soil heavy metal contamination and risk assessment around the Fenhe Reservoir, China. *Bull. Environ. Contam. Toxicol.* **2014**, *93*, 182–186. [[CrossRef](#)]
6. Mehmood, A.; Raza, W.; Kim, K.H.; Raza, N.; Lee, S.S.; Zhang, M.; Lee, J.; Sarfraz, M. Spatial distribution of heavy metal in crops in a wastewater irrigated zone and health risk assessment. *Environ. Res.* **2019**, *168*, 382–388. [[CrossRef](#)]
7. Stafilov, T.; Šajin, R.; Boev, B.; Cvetković, J.; Mukaetov, D.; Andreevski, M.; Lepitkova, S. Distribution of some elements in surface soil over the Kavadarci region, Republic of Macedonia. *Environ. Earth Sci.* **2010**, *61*, 1515–1530. [[CrossRef](#)]
8. Song, H.Y.; Hu, K.L.; An, Y.; Chen, C.; Li, G.D. Spatial distribution and source apportionment of the heavy metals in the agricultural soil in a regional scale. *J. Soils Sediments* **2018**, *18*, 852–862. [[CrossRef](#)]
9. Shi, T.; Ma, J.; Wu, X.; Ju, T.; Lin, X.; Zhang, Y.; Li, X.; Gong, Y.; Hou, H.; Zhao, L.; et al. Inventories of heavy metal inputs and outputs to and from agricultural soils: A review. *Ecotoxicol. Environ. Safe* **2018**, *164*, 118–124. [[CrossRef](#)]
10. Kheir, A.M.; Ali, E.F.; Ahmed, M.; Eissa, M.A.; Majrashi, A.; Ali, O.A. Biochar blended humate and vermicompost enhanced immobilization of heavy metals, improved wheat productivity, and minimized human health risks in different contaminated environments. *J. Environ. Chem. Eng.* **2021**, *9*, 105700. [[CrossRef](#)]
11. Peng, T.; Wang, S. Effects of land use, land cover and rainfall regimes on the surface runoff and soil loss on karst slopes in southwest China. *Catena* **2012**, *90*, 53–62. [[CrossRef](#)]
12. Ma, L.; Sun, J.; Yang, Z.; Wang, L. Heavy metal contamination of agricultural soils affected by mining activities around the Ganxi River in Chenzhou, Southern China. *Environ. Monit. Assess.* **2015**, *187*, 731. [[CrossRef](#)]
13. Shetaya, W.H.; Marzouk, E.R.; Mohamed, E.F.; Elkassas, M.; Bailey, E.H.; Young, S.D. Lead in Egyptian soils: Origin, reactivity and bioavailability measured by stable isotope dilution. *Sci. Total Environ.* **2018**, *618*, 460–468. [[CrossRef](#)] [[PubMed](#)]
14. Wu, W.H.; Qu, S.Y.; Nel, W.; Ji, J.F. The impact of natural weathering and mining on heavy metal accumulation in the karst areas of the Pearl River Basin, China. *Sci. Total Environ.* **2020**, *734*, 139480. [[CrossRef](#)] [[PubMed](#)]
15. Kong, X.Y.; Liu, T.; Yu, Z.H.; Chen, Z.; Lei, D.; Wang, Z.W.; Zhang, H.; Li, Q.H.; Zhang, S.S. Heavy metal bioaccumulation in rice from a high geological background area in Guizhou Province, China. *Int. J. Environ. Res. Public Health* **2018**, *15*, 2281. [[CrossRef](#)]
16. Sahoo, P.K.; Dall’Agnol, R.; Salomão, G.N.; Junior, J.D.S.F.; da Silva, M.S.; Martins, G.C.; Filho, P.W.M.S.; Powell, M.A.; Maurity, C.W.; Angelica, R.S.; et al. Source and background threshold values of potentially toxic elements in soils by multivariate statistics and GIS-based mapping: A high density sampling survey in the Parauapebas basin, Brazilian Amazon. *Environ. Geochem. Health* **2020**, *42*, 255–282. [[CrossRef](#)]
17. Sahoo, P.K.; Dall’Agnol, R.; Salomão, G.N.; Junior, J.D.S.F.; Silva, M.S.; Filho, P.W.M.; Costa, M.F.C.; Guilherme, L.R.G.; Siqueira, J.O. Regional-scale mapping for determining geochemical background values in soils of the Itacaiúnas River Basin, Brazil: The use of compositional data analysis (CoDA). *Geoderma* **2020**, *376*, 114504. [[CrossRef](#)]
18. Li, F.P.; Liu, W.; Lu, Z.B.; Mao, L.C.; Xiao, Y.H. A multi-criteria evaluation system for arable land resource assessment. *Environ. Monit. Assess.* **2020**, *192*, 79. [[CrossRef](#)]
19. Cai, L.M.; Xu, Z.C.; Ren, M.Z.; Guo, Q.W.; Xu, X.B.; Hu, G.C.; Wan, H.F.; Peng, P.G. Source identification of eight hazardous heavy metals in agricultural soils of Huizhou, Guangdong Province, China. *Ecotoxicol. Environ. Safe* **2012**, *78*, 2–8. [[CrossRef](#)] [[PubMed](#)]
20. Liu, M.; Han, Z.; Yang, Y. Accumulation, temporal variation, source apportionment and risk assessment of heavy metals in agricultural soils from the middle reaches of Fenhe River basin, North China. *RSC Adv.* **2019**, *9*, 21893–21902. [[CrossRef](#)]
21. Wang, S.S.; Sun, B.Y.; Li, C.D.; Li, Z.B.; Ma, B. Runoff and soil erosion on slope Cropland: A Review. *J. Resour. Ecol.* **2018**, *9*, 461–470.
22. Xia, L.Z.; Hoermann, G.; Ma, L.; Yang, L.Z. Reducing nitrogen and phosphorus losses from arable slope land with contour hedgerows and perennial alfalfa mulching in Three Gorges Area, China. *Catena* **2013**, *110*, 86–94. [[CrossRef](#)]
23. Ouyang, W.; Wu, Y.; Hao, Z.; Zhang, Q.; Bu, Q.; Gao, X. Combined impacts of land use and soil property changes on soil erosion in a mollisol area under long-term agricultural development. *Sci. Total Environ.* **2018**, *613*, 798–809. [[CrossRef](#)]
24. CNEMC (China National Environmental Monitoring Center). *The Soil Background Value in China*; China Environmental Science Press: Beijing, China, 1990.
25. Müller, G. Index of Geoaccumulation in Sediments of the Rhine River. *Geojournal* **1969**, *2*, 108–118.
26. Bhuiyan, M.A.H.; Parvez, L.; Islam, M.A.; Dampare, S.B.; Suzuki, S. Heavy metal pollution of coal mine-affected agricultural soils in the northern part of Bangladesh. *J. Hazard Mater.* **2010**, *173*, 384–392. [[CrossRef](#)] [[PubMed](#)]
27. Hakanson, L. An ecological risk index for aquatic pollution control. A sedimentological approach. *Water Res.* **1980**, *14*, 975–1001. [[CrossRef](#)]

28. Wang, N.; Wang, A.; Kong, L.; He, M. Calculation and application of Sb toxicity coefficient for potential ecological risk assessment. *Sci. Total Environ.* **2018**, *610*, 167–174. [[CrossRef](#)]
29. Andriyanto, C.; Sudarto, S.; Suprayogo, D. Estimation of soil erosion for a sustainable land use planning: RUSLE model validation by remote sensing data utilization in the Kalikonto watershed. *JDMLM* **2015**, *3*, 459–468.
30. Renard, K.G.; Foster, G.R.; Weesies, G.A.; McCool, D.K.; Yoder, D.C. *Predicting Soil Erosion by Water: A Guide to Conservation Planning with the Revised Universal Soil Loss Equation (RUSLE)*; USDA Handbook No. 703; United States Government Printing Office: Washington, DC, USA, 1997; pp. 1–251.
31. Fu, B.; Liu, Y.; Lu, Y.H.; He, C.S.; Zeng, Y.; Wu, B.F. Assessing the soil erosion control service of ecosystems change in the Loess Plateau of China. *Ecol. Complex.* **2011**, *8*, 284–293. [[CrossRef](#)]
32. Van Rompaey, A.J.; Verstraeten, G.; Van Oost, K.; Govers, G.; Poesen, J. Modelling mean annual sediment yield using a distributed approach. *Earth Surf. Process Landf.* **2001**, *26*, 1221–1236. [[CrossRef](#)]
33. Zhang, F.; Shen, C.Y.; Wang, S.F.; Jia, Y.F. Application of the RUSLE for determining Riverine heavy metal flux in the Upper Pearl River Basin, China. *Bull. Environ. Contam. Toxicol.* **2020**, *106*, 24–32. [[CrossRef](#)] [[PubMed](#)]
34. Vente, J.D.; Poesen, J.; Verstraeten, G.; Govers, G.; Vanmaercke, M.; Rompaey, A.V.; Arabkhedri, M.; Boix-Fayos, C. Predicting soil erosion and sediment yield at regional scales: Where do we stand. *Earth Sci. Rev.* **2013**, *127*, 16–29. [[CrossRef](#)]
35. Hamel, P.; Chaplin-Kramer, R.; Sim, S.; Mueller, C. A new approach to modeling the sediment retention service (InVEST 3.0): Case study of the Cape Fear catchment, North Carolina, USA. *Sci. Total Environ.* **2015**, *524–525*, 166–177. [[CrossRef](#)] [[PubMed](#)]
36. Wischmeier, W.H. A soil erodibility nomograph for farmland and construction sites. *J. Soil Conserv.* **1971**, *26*, 189–193.
37. Sharpley, A.N.; Williams, J.R. *EPIC-Erosion/Productivity Impact Calculator: 1. Model Determination*; U.S. Department of Agriculture: Washington, DC, USA, 1990.
38. Wischmeier, W.H.; Smith, D.D. *Predicting Rainfall Erosion Losses: A Guide to Conservation Planning (No. 537)*; Department of Agriculture, Science and Education Administration: Washington, DC, USA, 1978.
39. McCool, D.K.; Brown, L.C.; Foster, G.R.; Mutchler, C.K.; Meyer, L.D. Revised slope steepness factor for the Universal Soil Loss Equation. *Trans. ASAE* **1987**, *30*, 1387–1396. [[CrossRef](#)]
40. Liu, B.Y.; Nearing, M.A.; Risse, L.M. Slope gradient effects on soil loss for steep slopes. *Trans. ASAE* **1994**, *37*, 1835–1840. [[CrossRef](#)]
41. Cai, C.F.; Ding, S.W.; Shi, Z.H.; Huang, L.; Zhang, G.Y. Study of applying USLE and geographical information system IDRISI to predict soil erosion in small watershed. *J. Soil Water Conserv.* **2000**, *14*, 19–24, (In Chinese with English abstract).
42. Chen, Z.J.; Liu, S.Q.; Yang, D.G.; Chen, G.J. Soil and water loss and its controlling countermeasures in the upper reaches of the Yangtze River. *J. Soil Water Conserv.* **2000**, *14*, 1–5, (In Chinese with English abstract).
43. Yang, S.H.; Qu, Y.J.; Ma, J.; Liu, L.L.; Wu, H.W.; Liu, Q.Y.; Gong, Y.W.; Chen, Y.X.; Wu, Y.H. Comparison of the concentrations, sources, and distributions of heavy metal(loid)s in agricultural soils of two provinces in the Yangtze River Delta, China. *Environ. Pollut.* **2020**, *264*, 114688. [[CrossRef](#)]
44. Sun, R.G.; Yang, J.; Xia, P.H.; Wu, S.L.; Lin, T.; Yi, Y. Contamination features and ecological risks of heavy metals in the farmland along shoreline of Caohai plateau wetland, China. *Chemosphere* **2020**, *254*, 126828. [[CrossRef](#)]
45. Qin, F.X.; Wei, C.F.; Zhong, S.Q.; Huang, X.F.; Pang, W.P.; Jiang, X. Soil heavy metal(loid)s and risk assessment in vicinity of a coal mining area from southwest Guizhou, China. *J. Cent. South Univ.* **2016**, *23*, 2205–2213. [[CrossRef](#)]
46. Yuan, X.; Xue, N.; Han, Z. A meta-analysis of heavy metals pollution in farmland and urban soils in China over the past 20 years. *J. Environ. Sci.* **2021**, *101*, 217–226. [[CrossRef](#)]
47. He, M.C.; Wang, X.Q.; Wu, F.C.; Fu, Z.Y. Antimony pollution in China. *Sci. Total Environ.* **2012**, *421*, 41–50. [[CrossRef](#)]
48. Zhang, G.P.; Liu, C.Q.; Liu, H.; Hu, J.; Han, G.L.; Li, L. Mobilisation and transport of arsenic and antimony in the adjacent environment of Yata gold mine, Guizhou province, China. *J. Environ. Monitor.* **2009**, *11*, 1570–1578. [[CrossRef](#)]
49. Okkenhaug, G.; Zhu, Y.G.; He, J.; Li, X.; Luo, L.; Mulder, J. Antimony (Sb) and arsenic (As) in Sb mining impacted paddy soil from Xikuangshan, China: Differences in mechanisms controlling soil sequestration and uptake in rice. *Environ. Sci. Technol.* **2012**, *46*, 3155–3162. [[CrossRef](#)]
50. Tu, C.L.; He, T.B.; Liu, C.Q.; Lu, X.H. Effects of Land Use and Parent Materials on Trace Elements Accumulation in Topsoil. *J. Environ. Qual.* **2013**, *42*, 103–110. [[CrossRef](#)]
51. Shan, Y.S.; Tysklind, M.; Hao, F.H.; Ouyang, W.; Chen, S.Y.; Lin, C.Y. Identification of sources of heavy metals in agricultural soils using multivariate analysis and GIS. *J. Soils Sediments* **2013**, *13*, 720–729. [[CrossRef](#)]
52. Rao, E.M.; Xiao, Y.; Ouyang, Z.Y.; Yu, X.X. National assessment of soil erosion and its spatial patterns in China. *Ecosyst. Health Sust.* **2015**, *1*, 1–10. [[CrossRef](#)]
53. Sun, Y.; Li, H.; Guo, G.; Semple, K.T.; Jones, K.C. Soil contamination in China: Current priorities, defining background levels and standards for heavy metals. *J. Environ. Manag.* **2019**, *251*, 109512. [[CrossRef](#)]
54. Xia, J.; Luo, Y. Definition and three evaluation guidelines of soil contamination. *J. Ecol. R. Environ.* **2006**, *22*, 87–90.
55. Stephen, G.P.; Huang, J.Z.; Li, Z.P.; Jing, C.G. Sedimentary rock-hosted Au deposits of the Dian–Qian–Gui area, Guizhou, and Yunnan Provinces, and Guangxi District, China. *Ore Geol. Rev.* **2007**, *31*, 170–204.
56. Wu, W.H.; Qu, S.Y.; Nel, W.; Ji, J.F. The influence of natural weathering on the behavior of heavy metals in small basaltic watersheds: A comparative study from different regions in China. *Chemosphere* **2021**, *262*, 127897. [[CrossRef](#)]

57. Quinton, J.N.; Catt, J.A. Enrichment of heavy metals in sediment resulting from soil erosion on agricultural fields. *Environ. Sci. Technol.* **2007**, *41*, 3495–3500. [[CrossRef](#)]
58. Borrelli, P.; Robinson, D.A.; Fleischer, L.R.; Lugato, E.; Ballabio, C.; Alewell, C.; Meusburger, K.; Modugno, S.; Schütt, B.; Ferro, V.; et al. An assessment of the global impact of 21st century land use change on soil erosion. *Nat. Commun.* **2017**, *8*, 2013. [[CrossRef](#)]
59. Zhang, F.; Zhang, X.; Bi, Z.; Yu, Y.; Shi, P.; Ren, L.; Shan, Z. The impact of land use changes and erosion process on heavy metal distribution in the hilly area of the Loess Plateau, China. *Sci. Total Environ.* **2020**, *718*, 137305. [[CrossRef](#)]
60. Fu, B.J.; Wang, Y.F.; Lü, Y.H.; He, C.S.; Chen, L.D.; Song, C.J. The effects of land-use combinations on soil erosion: A case study in the Loess Plateau of China. *Prog. Phys. Geogr.* **2009**, *33*, 793–804. [[CrossRef](#)]
61. Mao, L.C.; Liu, L.B.; Yan, N.X.; Li, F.P.; Tao, H.; Ye, H.; Wen, H.F. Factors controlling the accumulation and ecological risk of trace metal(loid)s in river sediments in agricultural field. *Chemosphere* **2020**, *243*, 125359. [[CrossRef](#)]
62. Shi, P.; Zhang, Y.; Zhang, Y.; Yu, Y.; Li, P.; Li, Z.; Xiao, L.; Xu, G.; Zhu, T. Land-use types and slope topography affect the soil labile carbon fractions in the Loess hilly-gully area of Shaanxi, China. *Arch. Agron. Soil Sci.* **2019**, *66*, 638–650. [[CrossRef](#)]
63. Basta, N.T.; Pantone, D.J.; Tabatabai, M.A. Path analysis of heavy metal adsorption by soil. *Agron. J.* **1993**, *85*, 1054–1057. [[CrossRef](#)]
64. Shetaya, W.H.; Huang, J.H.; Osterwalder, S.; Mestrot, A.; Bigalke, M.; Alewell, C. Sorption kinetics of isotopically labelled divalent mercury ($^{196}\text{Hg}^{2+}$) in soil. *Chemosphere* **2019**, *221*, 193–202. [[CrossRef](#)]